sustainability

MDPI

Article

Use of GIS Tools in Sustainable Heritage Management—The Importance of Data Generalization in Spatial Modeling

Mateusz Ciski *, **Krzysztof Rząsa** and **Marek Ogryzek**

The Faculty of Geodesy, Geospatial and Civil Engineering, Institute of Geography and Land Management, University of Warmia and Mazury in Olsztyn, Prawocheńskiego Street 15, 10-720 Olsztyn, Poland; krzysztof.rzasa@uwm.edu.pl (K.R.); marek.ogryzek@uwm.edu.pl (M.O.)

* Correspondence: mateusz.ciski@uwm.edu.pl

Received: 2 August 2019; Accepted: 8 October 2019; Published: 12 October 2019

check for updates

Abstract: Cultural heritage is a very important element affecting the sustainable development. To analyze the various forms of spatial management inscribed into sustainable development, information on the location of objects and their concentration at specific areas is necessary. The main goal of the article was to show the possibility of using various GIS tools in modeling the distribution of historical objects. For spatial analysis, it is optimal to use the point location of objects. Often, however, it is extremely difficult, laborious, expensive, and sometimes impossible to obtain. Thus, various map content generalizations were analyzed in the article; the main goal was to find the level for which the data with an acceptable loss of accuracy can be generalized. Such analyses can be extremely useful in sustainable heritage management. Article also shows how cultural heritage fits into the sustainable heritage management. The research included non-movable monuments in Poland. The obtained results showed the universality of this type of research both in the thematic sense (can be used for various types of objects) and spatial sense (can be performed locally, at the country level, or even at the continental level).

Keywords: cultural heritage; sustainable heritage management; GIS; geographic information system; hexagonal grid; data generalization

1. Introduction

Sustainable development is nowadays one of the main components used in spatial development [1–3]. It is considered a Constitutional Principle of the Republic of Poland, as well as in another European countries. The definition of sustainable development can be found in Polish legislation—it is defined in the Environmental Protection Act [4] as the socio-economic development integrating political, economic, and social actions, balanced with environmental protection and a permanence of basic natural processes, in order to ensure the possibility of satisfying the basic needs of communities or individual citizens in both the present and future generations. In The Brundtland Report "Our Common Future" [5] sustainable development is defined as "development that meets the needs of the present without compromising the ability of future generations to meet their own needs". The report highlighted three fundamental components of sustainable development: environmental protection, economic growth, and social equity. According to Pearce and Turner [6], sustainable development is associated with maximizing the benefits of economic development, in connection with protecting the quality and usability of natural resources. Such economic development must not only mean an increase in income per capita, but also the comprehensive improvement of other social aspects. Culture, as the basis of social life, is considered to be one of the four pillars of sustainable development [7–10]. Culture can be both the goal of development of a given society as well as the method of that development, but above all it is the development regulator [11]. Cultural heritage is one of the main elements of such described culture and it is understood much more broadly than just in the field of the protection of monuments, it also consists of: local traditions and customs, cultural affiliation or the sources of non-material values [12–14]. A greater sense of cultural identity can also contribute to the further development of social capital, because individuals and communities with a stronger sense of place are more actively involved in social matters. People living in places with a higher concentration of significant historical areas tend to have a stronger sense of place and/or increased social capital [15]. Cultural heritage is traditionally regarded as a non-economic factor of spatial development. However, treated as a resource and properly managed, it can be transformed into capital that can play an important role in the sustainable development strategies, both at the local and national level. The term "cultural heritage" covers a broad spectrum of meanings that are not obvious and can be ambiguous [16]. Cultural heritage is important as a source of remembrance and inspiration, and at the same time contributes to national and local identity, which is essential for sense of place and social cohesion [17]. Various studies have shown the influence of cultural heritage as an element of sustainable development on spatial planning [18,19], or tourism development [20–22].

To properly manage cultural heritage within sustainable development, regardless of the specific goal, knowledge of the location of objects constituting a material element of cultural heritage is necessary. In this article, the starting point for the conducted research and analyses were non-movable monuments in Poland. The legal basis for the protection of monuments in Poland is the Act of 23 July 2003 on the protection of monument and the care of monuments [23]. According to Article 3 of the above-mentioned Act, a non-movable monument is a real estate, its part or a complex of real estate, which is the work of humankind or is related to its activity, and is a testimony to a past era or event; whose protection is in the public interest because of its historical, artistic or scientific value. Article 6 of the Act indicates that non-movable monuments may include: cultural landscapes, urban and rural systems, building units, works of architecture and construction, works of defense construction; technical objects; cemeteries; parks, gardens, and other forms of designed greenery; as well as places commemorating historical events or the activities of remarkable characters or institutions. Non-movable monuments are registered by entry in "the register of objects of cultural heritage" (pol. rejestr zabytków), kept by the Voivodeship Conservators of Monuments. Voivodeship registers of objects of cultural heritage currently contain approx. 85 thousand entries on non-movable monuments, diversified in terms of type. A non-movable monument can be entered into the register on the basis of: an ex-officio decision issued by the Voivodeship Conservator of Monuments, or at the request of the owner of the non-movable monument or perpetual usufructuary of the land on which the non-movable monument is located. In the conducted research, the authors used data obtained from The National Heritage Board of Poland. The National Heritage Board of Poland (NHBP) is a cultural institution established by the Minister of Culture and National Heritage; its present structure was formed in 2007. NHBP is a state agency that gathers and disseminates information on heritage, sets standards for its protection and conservation, and aims to raise the social awareness on cultural heritage of Poland in order to save it for future generations in accordance with the strategy for sustainable development. The generic division of non-movable monuments used by NHBP is shown in the Figure 1.

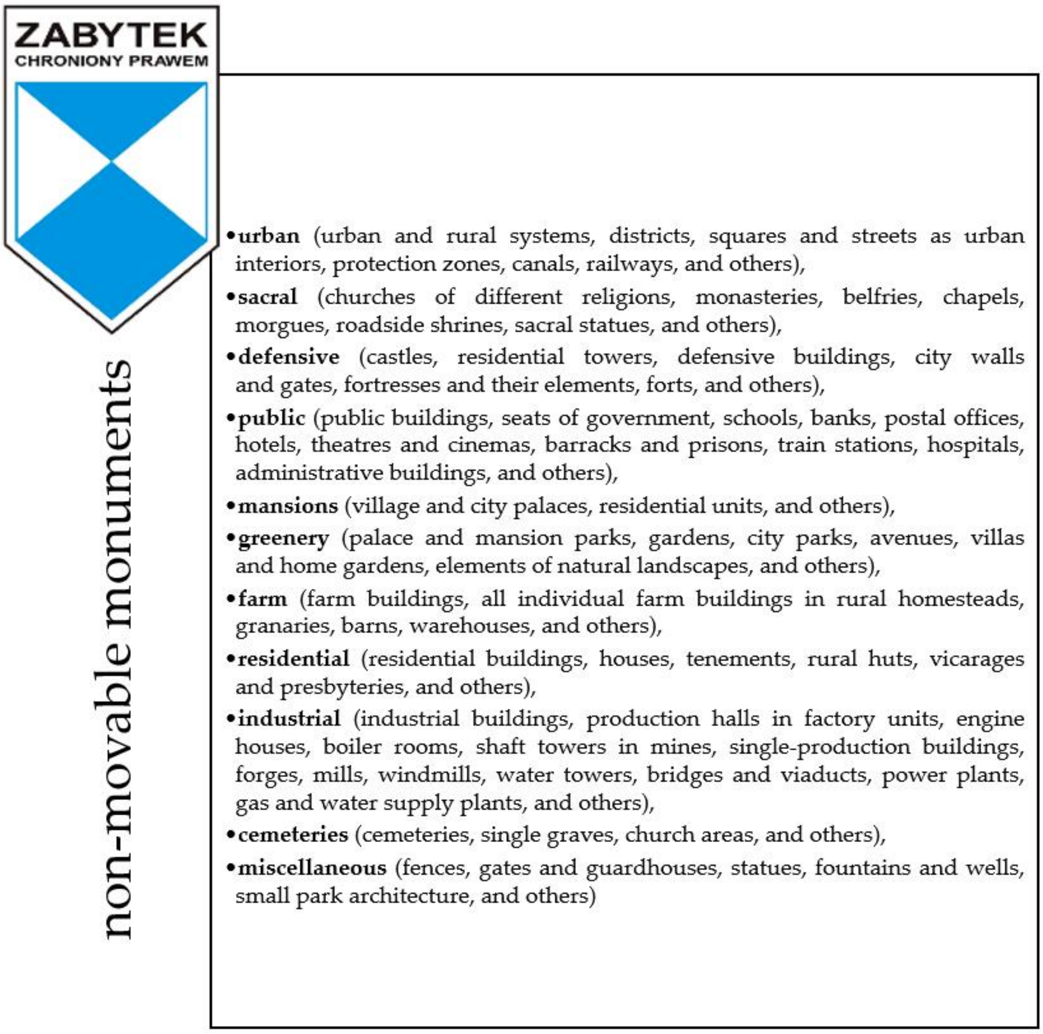

Figure 1. Types of non-movable monuments in Poland. Own elaboration using information from [23] and information sign "Monument protected by law" (pol. Zabytek chroniony prawem). Non-movable monuments entered in the register of monuments are marked by this sign, it is an international symbol of cultural heritage protection, the sign of the Blue Shield [24]. The description of the sign was included in the 1954 Hague Convention [25], for the protection of monuments during armed conflicts, and the originator of the graphic form and its author was the Polish architect, prof. Jan Zachwatowicz.

When determining the location of individual monuments, reference was made to the administrative division of Poland. This division includes [26]:

- 16 voivodeships,
- 314 poviats and 66 cities with poviat rights,
- 2477 municipalities (including 302 urban municipalities, 638 urban–rural municipalities, and 1537 rural municipalities).

The spatial distribution of the administrative division of Poland is shown in the Figure 2, and the quantitative data on the number of non-movable monuments in individual voivodeships in 2018—in Figure 3.

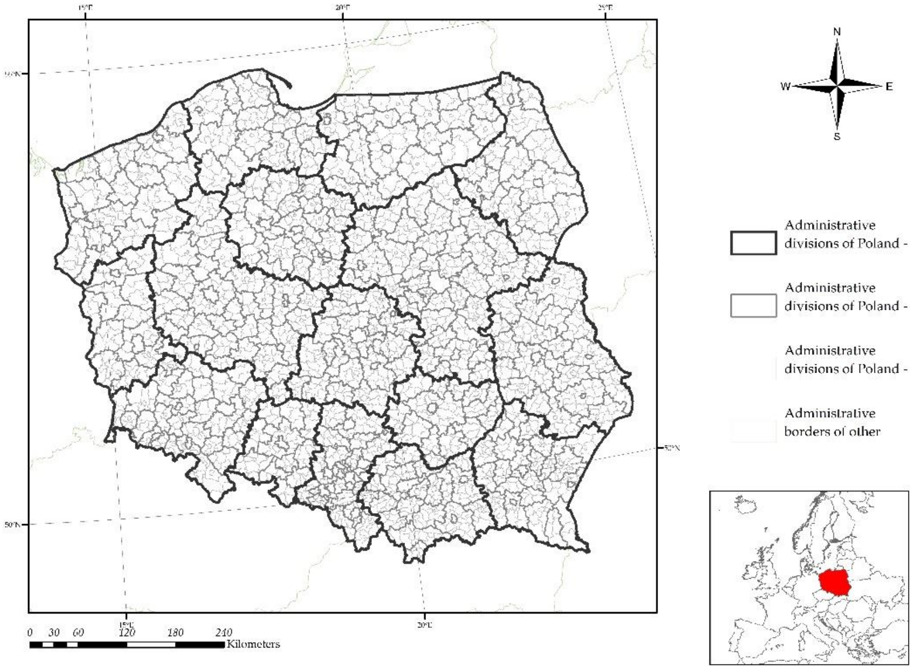

Figure 2. Administrative divisions of Poland (with illustrative map of Poland's location in Europe). Own elaboration using ArcMap component of ArcGIS 10.6, on the basis of: world data from [27], polish administrative data from [28].

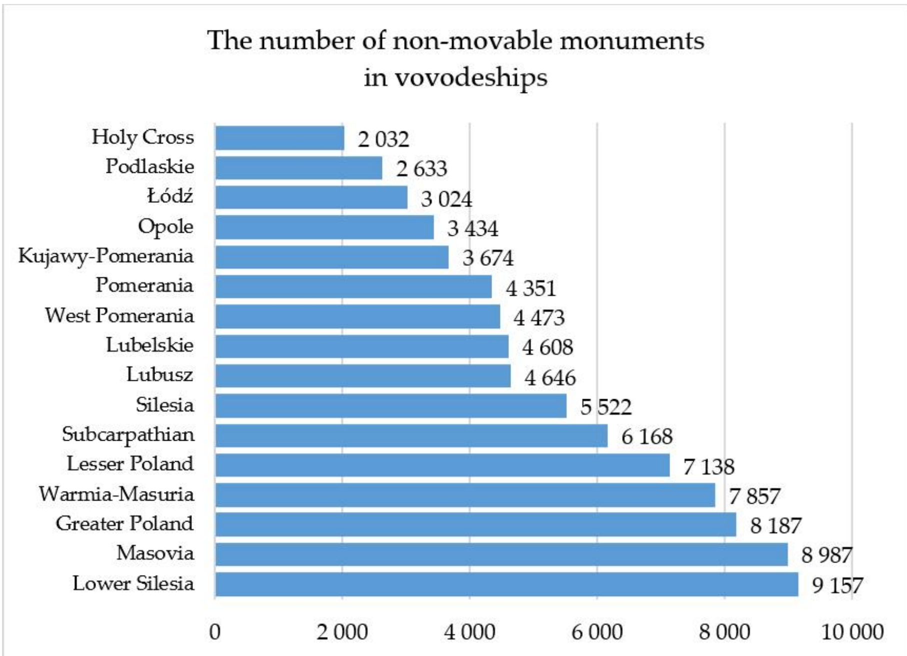

Figure 3. The number of non-movable monuments in voivodeships in Poland. Own elaboration using Microsoft Excel software, on the basis of: polish administrative data from [28], point data from NHBP.

After obtaining location and generic data of all non-movable monuments in Poland, the authors continued the research using the Geographic Information System (GIS). GIS is an information system used to enter, collect, process, and visualize geographic data. It is a powerful tool; spatial analyses using GIS significantly support decision-making processes. Spatial data for GIS can be obtained by, among others: field measurements, digitalization of analog data (including historical data), or three-dimensional photogrammetry digitization and other methods of photogrammetry and remote sensing. Additional data entry functions include: entering descriptive data, geometric construction, interactive editing of objects (removal, modification). Data management can be defined as a set of processes with the main purpose of keeping the information resources of the system in good condition. It is also important that the data structures and search mechanisms provides efficient information sharing. The processing functions include transforming, analyzing, aggregating, and generalizing. GIS software allows spatial analysis using a variety of methods, the most popular include: overlay analysis, spatial interpolation, spatial data exploration, hot spot analysis, or kernel density estimation; this type of research finds application in a number of areas, e.g., bathymetry [29], spatial planning [30], location selection [31,32], environmental protection and disaster reduction capability [33–37], spatial and distribution patterns [38–41], demography [42], as well as many others. Using GIS software, the data can be visualized using many cartographic visualization methods, such as: cartogram, cartodiagram, range method, dot map, etc. [43].

Analyses related to management (including sustainable heritage management) requires a reference to the spatial location of objects [44,45]. The optimal solution is to acquire point data, however, as indicated in the Section 2 Materials and Methods, in practice, visualization is applied at different levels of generalization. The aim of the conducted research was to find the grid size for which the data with an acceptable loss of accuracy can be generalized. The goal was achieved using GIS tools, confirming its usefulness in such analyses.

2. Materials and Methods

When conducting spatial analysis, the use of precise point or linear data is in the most cases a model situation and gives the possibility to obtain the most accurate, flexible results [46]. Having information about the exact location of the analyzed phenomena allows for an in-depth examination of the issue. However, the availability of such data is often a problem [47]. Usually it is caused by the cost of acquisition, laboriousness, or impossibility to carry out measurements, but can also be related to the object's specification. In the absence of precise data, some kind of generalization is introduced. Most often, data is collected for administrative division units. The smallest administrative division is usually sufficient for spatial analyses [48]. The main advantage of using administrative division units in spatial analysis is the availability of data collected in various types of offices (state, administrative)—it usually refers to administrative units [48]. The use of this type of units also simplifies the presentation of results to non-specialists (e.g., to local government authorities).

However, the administrative division units are spatially unequal, which increases difficulty of comparability (e.g., the smallest municipality in Poland has an area equal to 3.32 km^2, the largest—6444 km^2). The basic advantage of using geometric figures in spatial analyses is its identical surface, which facilitates comparability; it is also easy to develop it using digital techniques. The most popular geometric figures are: triangles, squares, and hexagons; these are the only regular shapes that tessellates the plane with no gaps [49]. In studies performed for the purposes of the article hexagonal grid was used—the higher usefulness of the hexagon over other figures has been repeatedly confirmed in the case of spatial analyses [50–52], as well as in other cases [53–57]. The aim of this research was to find the optimal size of the hexagonal grid, to the level of which the data can be generalized, without a significant decrease in the reliability of spatial modeling for various sustainable heritage management needs.

The practical part of the research was carried out in the Esri ArcGIS 10.6 software. All map attachments (as well as the entire practical part of the tests) were made in the Lambert Azimuthal Equal Area 52N 10E ETRS89 reference system. This projection accurately represents area in all regions of the sphere, but it does not accurately represent angles; it is commonly seen in atlases [58]. European Environment Agency (EEA) recommends the use of this reference system for storing raster data, for statistical analysis and for map display purposes (small scale mapping 1:500,000 or smaller applications) [59,60]. In the research, point data with the exact location of non-movable monuments in Poland, obtained from the National Heritage Board of Poland were used. The data has been verified and prepared for GIS analyses. The data describe the state on 1 August 2018, and contain the exact location and description of 85,891 non-movable monuments in Poland (Figure 4).

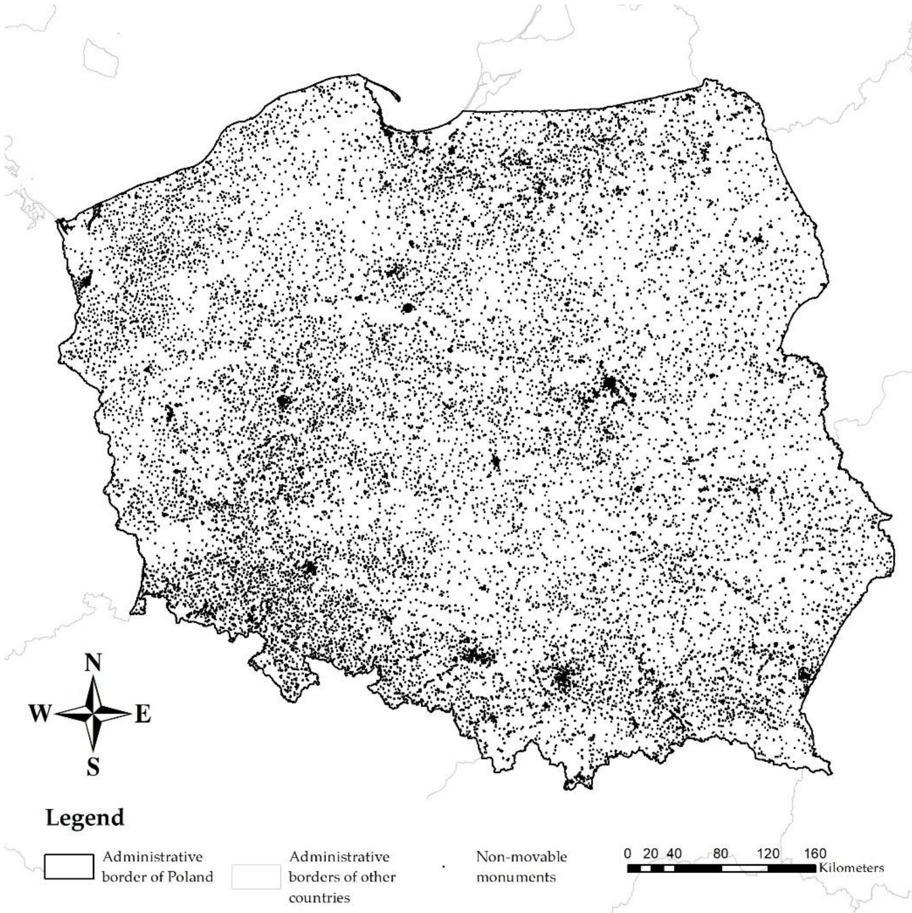

Figure 4. Location of non-movable monuments in Poland. Own elaboration using ArcMap component of ArcGIS 10.6, on the basis of: world data from [27], polish administrative data from [28], point data from NHBP.

The research has been divided into three main stages:

1. Stage I—Creating the map of the density of non-movable monuments with kernel density estimation
2. Stage II—Choosing the optimal method of spatial interpolation
3. Stage III—Finding the optimal size of the geometric grid

In the first stage, using the point data, a map of the density of non-movable monuments in Poland was created using kernel density estimation. Kernel density estimation (KDE) is an important method of spatial data visualization; KDE presents the density of the analyzed points in a given spatial extent [61], thus showing spatial patterns [62,63]. This is a non-parametric estimation, it directly uses point data [64]. KDE calculates the density of point features around each output raster cell. The surface value is highest at the location of the point and diminishes with increasing distance from the point, reaching zero at the search radius (or 'bandwidth') distance from the point. The kernel function is based on the quartic kernel function described in [61]. This method finds application in many fields of science, such as: archaeology [65,66], astronomy [67–71], biology [72–75], forecasting [76,77], environmental protection [78,79], medicine and health studies [80–83], and many others. Choosing the appropriate bandwidth in KDE is the subject of many studies [84–86]. If the bandwidth is too low (the impact range of the kernels is too small), KDE can give unsmooth density; while too-large a bandwidth can over-generalize the data, giving inaccurate picture [64]. The created map of the density of non-movable monuments in Poland will serve as a model image, to which maps created using generalized hexagons will be compared.

The second stage was to determine the optimal data visualization method for the analyzed dataset. The point data was combined with administrative division units—points contained in polygons were summed up, and assigned to appropriate polygons. Polygons were then visualized with cartogram method in order to present a spatial distribution of data. A cartogram is a very good cartographic visualization method, but it has a significant disadvantage—the need to classify data gives a distorted view of the continuity of value across the entire polygon in a specific class [43]. In order to obtain more accurate view of continuity, polygon data were converted to point data (polygon centroids), and then interpolated using nine spatial interpolation methods, available in the "Geostatistical Analyst" add-on of ArcGIS software: inverse distance weighting (IDW), global polynomial interpolation (GPI), radial basis function (RBF), local polynomial interpolation (LPI), ordinary kriging (OK), simple kriging (SK), universal kriging (UK), disjunctive kriging (DK), and empirical Bayesian kriging (EBK). Spatial interpolation effectively generates a full spatial attribute pattern in a large spatial range. This tool accurately creates a spatial pattern of attributes with spatial continuity [87]. Spatial interpolation is found useful in many fields of science, such as: environmental and pollution studies [88–91], soil science/pedology [92–95], hydrology [96], bathymetry [97,98], medicine and health studies [99,100], as well as many others. Kriging interpolation is a geostatistical method for estimating values at unmeasured locations, based on empirical spatial structure quantified in a semivariogram model [101]. The aim of this part of the research was to determine the optimal method of spatial interpolation for the analyzed data using cross-validation. The values at the measured points of the analyzed point layer were interpolated—this way, maps (models) with spatial continuity were obtained. Comparing the accuracy of these maps is possible using the difference between measured points and modeled points (cross-validation). These differences are errors that constitute the basic determinant of model accuracy. Interpolation methods were compared on the basis of root-mean-square-error (RMSE). RMSE is recommended for comparing spatial interpolation methods [102], a smaller error value means a better adjusted model [91,97]. On the basis of cross-validation, the optimal method for visualizing the analyzed data was chosen.

In the third stage, a geometric grid composed of hexagons was generated. The hexagonal grid was created using the ArcGIS 'Generate Tessellation' tool. For different sizes of hexagons, polygons were combined with point data (same as in the second stage) and then visualized using the chosen interpolation method. The aim of the research was to find the optimal grid size, to the level of which the data can be generalized without a significant decrease in the credibility of spatial modeling. The Pearson correlation coefficient, calculated for the density map of non-movable monuments from the first part of the study and for maps created from subsequent hexagon sizes, was selected as the reliability indicator. KDE allows to obtain density values at any point within the analysis range [103], similarly for all methods of spatial interpolation [87]. This feature was used to obtain tabular data necessary to calculate Pearson's correlation coefficient—but a point layer was needed, to collect the raster cell values. Test layers compose of randomly generated 8589 points (created using 'Create Random Points' tool), which corresponds with 10% of the complete set. To each particular point, the value of the chosen raster layer was assigned (from the model map created using KDE and a map created using the optimal interpolation method). Five test layers were applied, averaging Pearson's correlation coefficients for five measurements, thus obtaining more reliable results. Received tabular data was compared using the Pearson's correlation coefficient. In order to find the size of the hexagon for which the correlation coefficient is the highest, the above process was carried out for three levels of accuracy (every 10 km^2, 5 km^2, and 1 km^2), narrowing the scope of the analysis with each level. By comparing successive values of Pearson's correlation coefficient, one size of the hexagon was found, for which its value is the highest—it means finding the optimal grid size to which the data can be generalized without a significant decrease in reliability. Analyses carried out in this way allowed to draw conclusions in the field of the analyzed problem.

3. Results

3.1. Map of the Density of Non-Movable Monuments—Kernel Density Estimation

The 'Kernel Density' tool from ArcGIS software was used to generate a density map of non-movable monuments in Poland. The built-in algorithm for determining the optimal bandwidth was used—it is (around rounded up to thousands) 40 km. Figure 5 shows the density map of non-movable monuments in Poland, generated on the basis of point data obtained from NHBP, using the ArcGIS 'Kernel Density' tool.

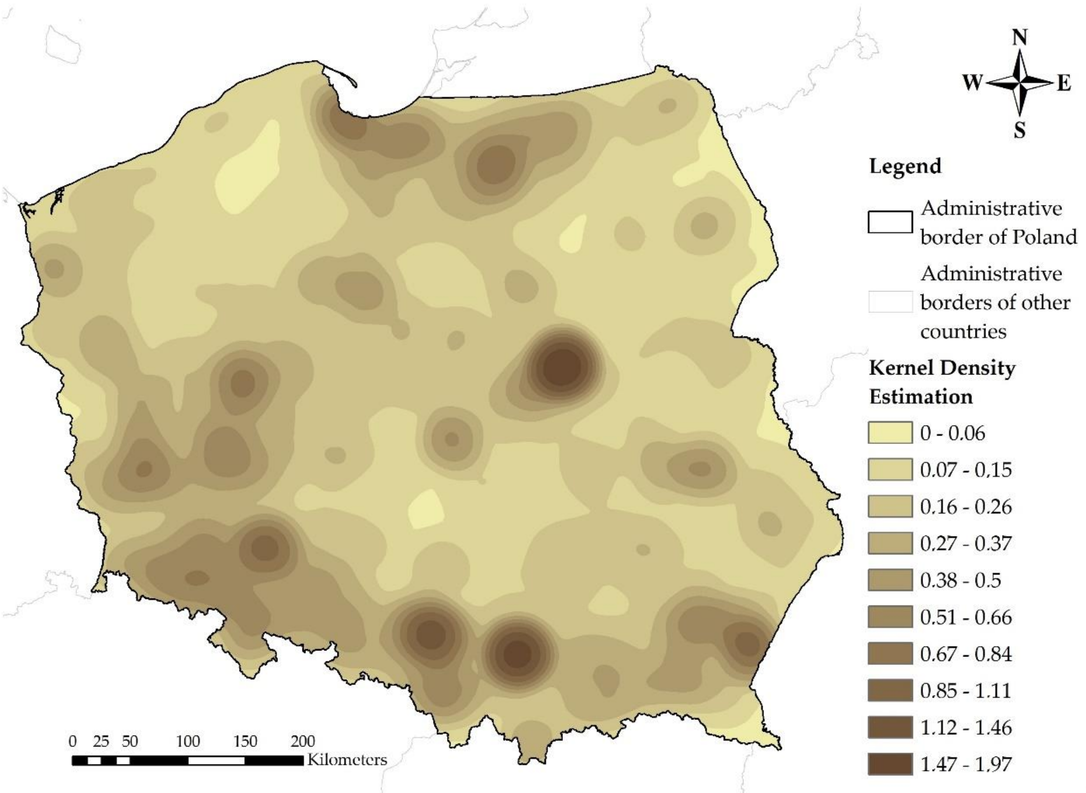

Figure 5. Map of the density of non-movable monuments in Poland. Own elaboration using ArcMap component of ArcGIS 10.6, on the basis of: world data from [27], point data from NHBP.

The generated Figure 5 will serve as a model image of the reality to which maps created using generalized hexagons will be compared. KDE allows to show the accurate spatial pattern, but as indicated in the Materials and Methods section, the availability of point data may be limited.

3.2. Optimal Method of Spatial Interpolation

Point data were combined with administrative division units, which were then visualized using a cartogram method (Figure 6).

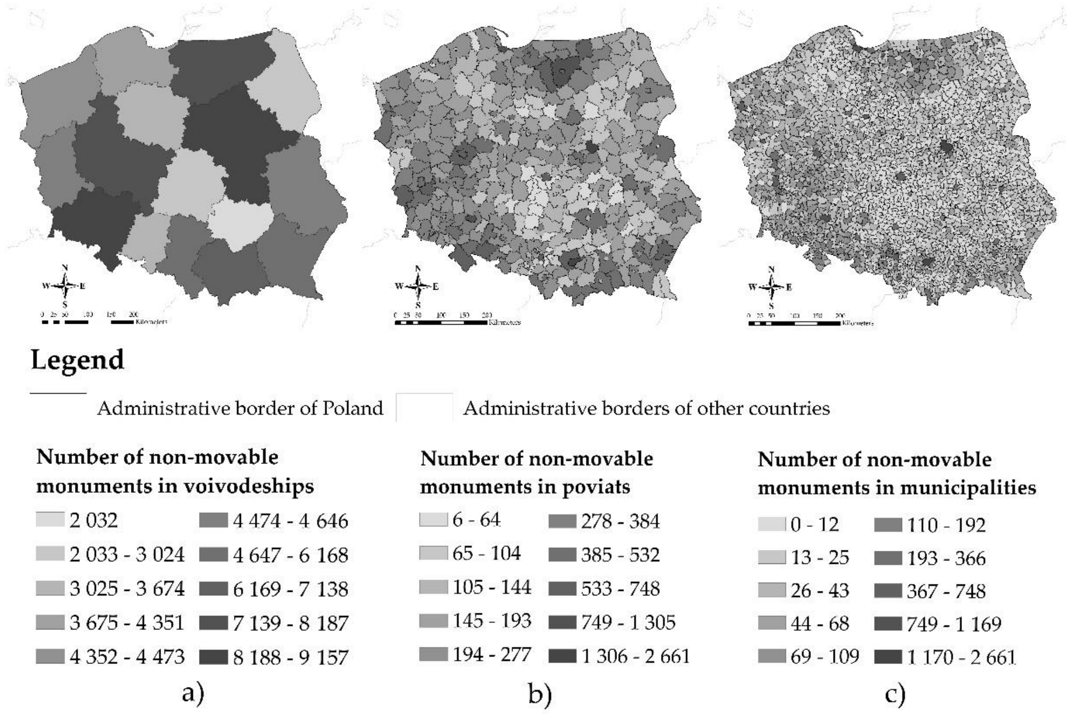

Figure 6. Number of non-movable monuments in administrative division units: (**a**) voivodeships, (**b**) poviats, (**c**) municipalities. Own elaboration using ArcMap component of ArcGIS 10.6, on the basis of: world data from [27], polish administrative data from [28], point data from NHBP.

For three levels of administrative division, data on the number of non-movable monuments in Poland were interpolated using the nine methods, as indicated in Materials and Methods. The information on RMSE was then collected, as shown in Table 1. Additional information on individual datasets is presented in Table 2.

Table 1. Collected root-mean-square errors. Own elaboration.

Interpolation Method	Voivodeships	Poviats	Municipalities
Inverse distance weighting (IDW)	2735.33	226.06	94.42
Global polynomial interpolation (GPI)	4709.37	231.23	91.86
Radial basis function (RBF)	2813.37	222.06	94.14
Local polynomial interpolation (LPI)	3672.84	225.64	91.77
Ordinary kriging (OK)	2477.61	230.30	96.06
Simple kriging (SK)	**2223.73**	**215.70**	**91.52**
Universal kriging (UK)	2477.61	228.88	95.89
Disjunctive kriging (DK)	2477.61	217.65	91.64
Empirical Bayesian kriging (EBK)	2538.04	226.01	94.42

Table 2. Additional information about individual data sets. Own elaboration.

Measure	Voivodeships	Poviats	Municipalities
Skewness	0.34	5.50	17.08
Kurtosis	1.85	49.21	408.73
Minimum	2032	6	0
Maximum	9157	2661	2661
Mean	5368.10	226.03	34.675
Standard deviation	2295.40	231.68	92.358

The average size of the voivodeship in Poland is 19,543.82 km^2; poviat—822.90 km^2; and municipality—126.24 km^2. Generalization in the case of the first two divisions is very large, which can be seen in the high error rates. When performing cross-validation and comparing obtained root-mean-square-errors, a clear result appears—the RMSE values are the lowest for simple kriging method (2223.73 for voivodeships, 215.70 for poviats, and 91.52 for municipalities). Simple kriging method demonstrates therefore the best adjustment of the model (values at the unmeasured locations are the closest to the values at the measured locations); this method was therefore chosen as optimal for subsequent tests. The results of spatial interpolation using the simple kriging method have been shown in the Figure 7.

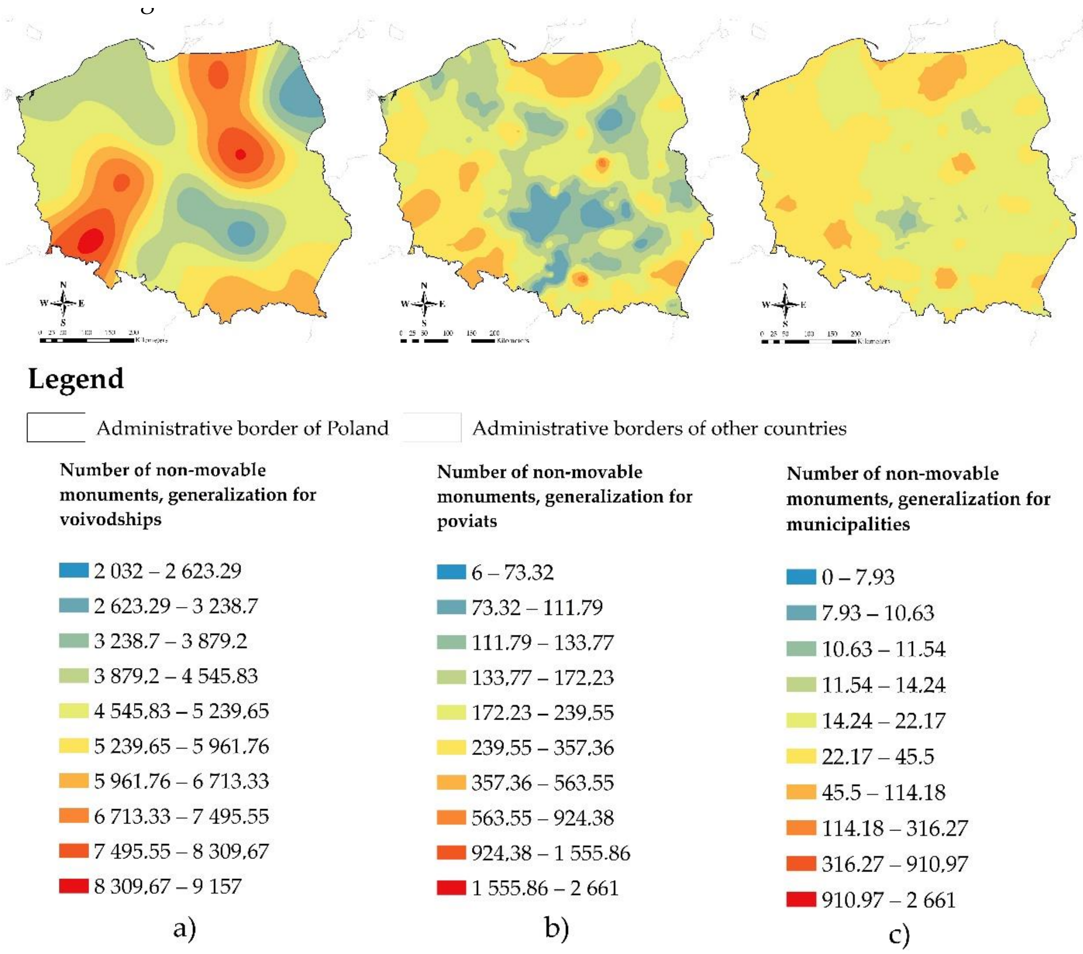

Figure 7. Number of non-movable monuments in Poland, simple kriging method, generalization for administrative division units: (**a**) voivodeships, (**b**) poviats, (**c**) municipalities. Own elaboration using ArcMap component of ArcGIS 10.6, on the basis of: world data from [27], polish administrative data from [28], point data from NHBP.

3.3. Optimal Size of the Geometric Grid

The last stage of the research was the analysis of data generalized to the series of generated hexagonal grids, in order to find the optimal grid size, to the level of which the data can be generalized without a significant decrease in reliability. The hexagonal grid was created using the ArcGIS 'Generate Tessellation' tool. Then, using the 'Spatial Join' tool, the values of the total number of points within its boundaries were assigned to the appropriate polygons. Polygon data has been converted to point data (using the 'Feature to Point' tool), and then it was interpolated using the simple kriging method. The above process, described in the ArcGIS ModelBuilder component, is shown in the Figure 8.

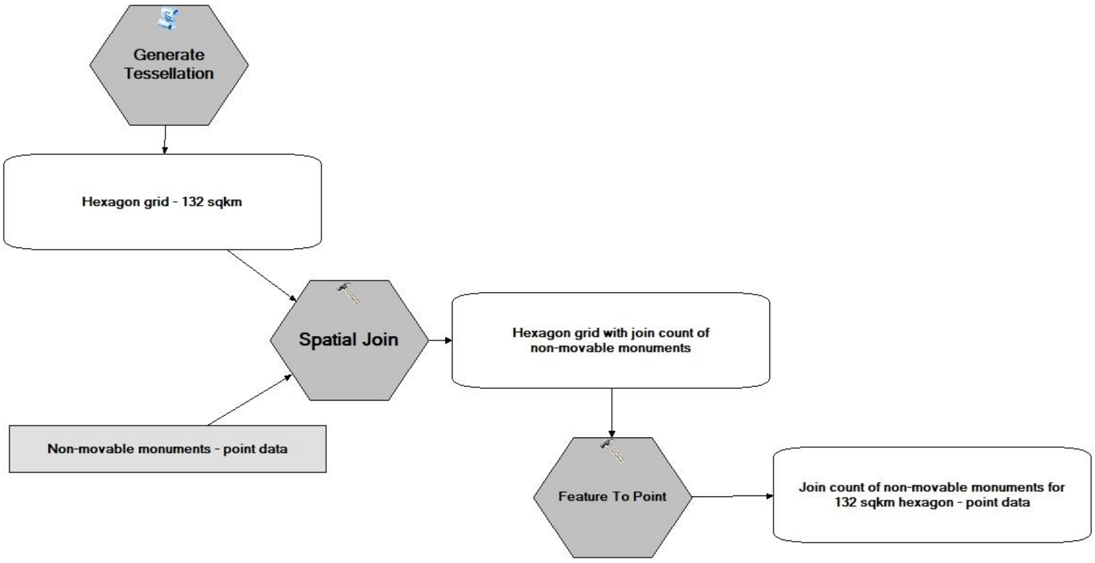

Figure 8. Model showing the process of generating a point layer to perform interpolation, based on a hexagon of a given size. Own elaboration using ArcMap component of ArcGIS 10.6.

The map created using the simple kriging method was compared to the map created using the 'Kernel Density' tool; The Pearson correlation coefficient was used as the indicator. The above process, described in the ArcGIS ModelBuilder component, is shown in the Figure 9.

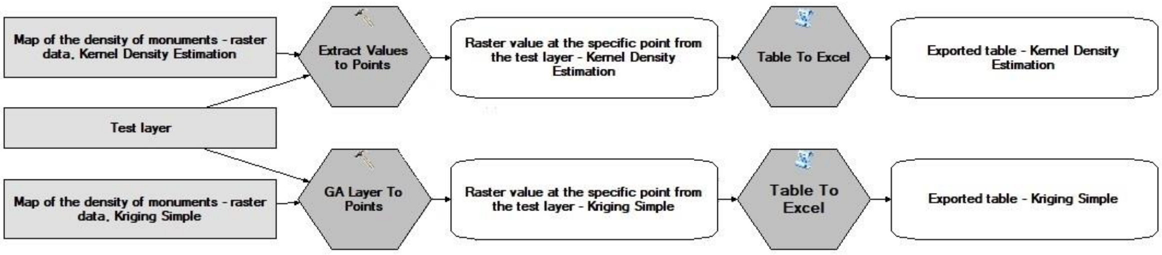

Figure 9. Model showing the process of assigning raster layer values to test points. Own elaboration using ArcMap component of ArcGIS 10.6.

In order to find the size of the hexagon for which the correlation coefficient is the highest, the processes described in Figures 8 and 9 were performed for three levels of accuracy (ranges of values)—every 10 km^2, 5 km^2, and 1 km^2—narrowing the scope of analysis with each level. On the first level of accuracy (10 km^2), hexagons were generated in the range of 10–300 km^2. The upper range was determined empirically on the basis of test research—higher values gave ever lower values of Pearson's correlation coefficient. Values of the correlation coefficient for particular hexagon sizes with an accuracy of 10 km are shown in the Table 3, and the distribution of mean values of the correlation coefficient in the Figure 10.

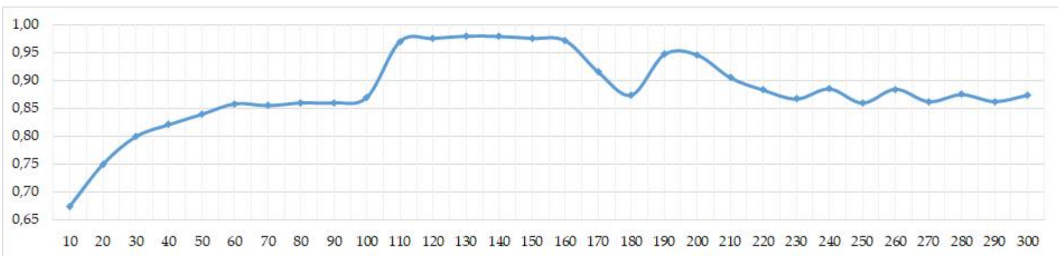

Figure 10. Mean values of Pearson's correlation coefficient, accuracy level 10 km^2. Own elaboration.

Table 3. Values of the correlation coefficient for particular sizes of hexagons, accuracy level 10 km^2. Own elaboration.

Hexagon Size	Test Layer 1	Test Layer 2	Test Layer 3	Test Layer 4	Test Layer 5	Mean
10	0.68	0.68	0.67	0.67	0.67	0.67
20	0.76	0.75	0.75	0.75	0.75	0.75
30	0.80	0.81	0.80	0.79	0.80	0.80
40	0.82	0.82	0.82	0.82	0.82	0.82
50	0.84	0.84	0.84	0.84	0.84	0.84
60	0.86	0.86	0.86	0.86	0.86	0.86
70	0.86	0.86	0.86	0.85	0.85	0.85
80	0.86	0.86	0.86	0.86	0.86	0.86
90	0.86	0.86	0.86	0.85	0.86	0.86
100	0.87	0.87	0.87	0.87	0.87	0.87
110	***0.97***	***0.97***	***0.97***	***0.97***	***0.97***	***0.97***
120	***0.98***	***0.98***	***0.98***	***0.97***	***0.97***	***0.98***
130	***0.98***	***0.98***	***0.98***	***0.98***	***0.98***	***0.98***
140	***0.98***	***0.98***	***0.98***	***0.98***	***0.98***	***0.98***
150	***0.98***	***0.98***	***0.98***	***0.98***	***0.97***	***0.98***
160	***0.97***	***0.97***	***0.97***	***0.97***	***0.97***	***0.97***
170	***0.91***	***0.92***	***0.92***	***0.91***	***0.91***	***0.92***
180	***0.87***	***0.87***	***0.88***	***0.87***	***0.88***	***0.87***
190	***0.95***	***0.95***	***0.95***	***0.94***	***0.95***	***0.95***
200	***0.95***	***0.95***	***0.95***	***0.95***	***0.94***	***0.95***
210	0.90	0.91	0.91	0.90	0.90	0.90
220	0.88	0.88	0.88	0.88	0.88	0.88
230	0.87	0.87	0.87	0.86	0.87	0.87
240	0.89	0.89	0.88	0.88	0.88	0.88
250	0.86	0.86	0.86	0.86	0.86	0.86
260	0.89	0.89	0.89	0.88	0.88	0.88
270	0.86	0.86	0.86	0.86	0.86	0.86
280	0.88	0.87	0.88	0.87	0.87	0.87
290	0.86	0.87	0.87	0.86	0.86	0.86
300	0.87	0.87	0.88	0.87	0.87	0.87

All hexagon sizes are characterized by a high correlation coefficient, however, the range of 110–200 km contains values with a coefficient above 0.95 (rounded to the hundredth level). This range was chosen for the next stage—5 km^2 accuracy. Values of the correlation coefficient for particular sizes of hexagons at the accuracy of 5 km^2 are presented in the Table 4, and the distribution of the average values of the correlation coefficient in the Figure 11.

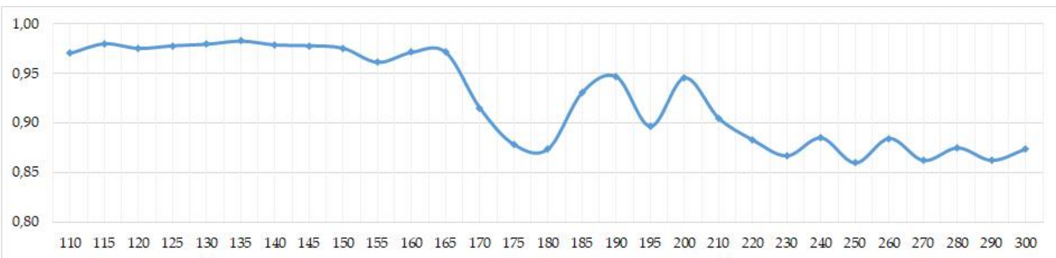

Figure 11. Mean values of Pearson's correlation coefficient, accuracy level 5 km^2. Own elaboration.

Table 4. Values of the correlation coefficient for particular sizes of hexagons, accuracy level 5 km^2. Own elaboration.

Hexagon Size	Test Layer 1	Test Layer 2	Test Layer 3	Test Layer 4	Test Layer 5	Mean
110	***0.970***	***0.972***	***0.971***	***0.971***	***0.968***	***0.970***
115	***0.979***	***0.979***	***0.981***	***0.981***	***0.980***	***0.980***
120	***0.976***	***0.976***	***0.977***	***0.974***	***0.974***	***0.975***
125	***0.978***	***0.979***	***0.978***	***0.978***	***0.977***	***0.978***
130	***0.979***	***0.981***	***0.980***	***0.980***	***0.978***	***0.980***
135	***0.983***	***0.984***	***0.983***	***0.983***	***0.982***	***0.983***
140	***0.979***	***0.980***	***0.980***	***0.979***	***0.977***	***0.979***
145	***0.979***	***0.978***	***0.979***	***0.978***	***0.977***	***0.978***
150	***0.976***	***0.975***	***0.976***	***0.977***	***0.974***	***0.976***
155	***0.962***	***0.963***	***0.960***	***0.962***	***0.960***	***0.961***
160	***0.972***	***0.972***	***0.971***	***0.971***	***0.971***	***0.971***
165	***0.971***	***0.970***	***0.972***	***0.972***	***0.971***	***0.971***
170	0.915	0.918	0.916	0.912	0.915	0.915
175	0.880	0.878	0.879	0.876	0.878	0.878
180	0.875	0.871	0.876	0.870	0.876	0.874
185	0.933	0.933	0.932	0.929	0.929	0.931
190	0.948	0.950	0.947	0.944	0.946	0.947
195	0.898	0.894	0.899	0.896	0.897	0.897
200	0.946	0.947	0.946	0.945	0.944	0.946

To the next level of accuracy (1 km^2) a range with a correlation coefficient higher than 0.970 (rounded up to the thousandth level) was selected—hexagons with an area of 110–165 km^2. Values of the correlation coefficient for particular sizes of hexagons at the accuracy of 5 km^2 are presented in the Table 5, and the distribution of the average values of the correlation coefficient in the Figure 12.

Table 5. Values of the correlation coefficient for particular sizes of hexagons, accuracy level 1 km^2. Own elaboration.

Hexagon Size	Test Layer 1	Test Layer 2	Test Layer 3	Test Layer 4	Test Layer 5	Mean
110	0.9699	0.9719	0.9711	0.9710	0.9685	0.9705
111	0.9689	0.9717	0.9702	0.9708	0.9681	0.9699
112	0.9717	0.9720	0.9726	0.9714	0.9705	0.9716
113	0.9802	0.9791	0.9785	0.9801	0.9799	0.9796
114	0.9762	0.9753	0.9755	0.9768	0.9742	0.9756
115	0.9795	0.9793	0.9811	0.9811	0.9795	0.9801
116	0.9809	0.9801	0.9810	0.9799	0.9786	0.9801
117	0.9779	0.9774	0.9784	0.9766	0.9766	0.9774
118	0.8564	0.8542	0.8532	0.8473	0.8514	0.8525
119	0.9793	0.9793	0.9802	0.9790	0.9777	0.9791
120	0.9761	0.9760	0.9767	0.9744	0.9738	0.9754
121	0.9780	0.9780	0.9798	0.9802	0.9769	0.9786
122	0.9778	0.9764	0.9779	0.9780	0.9746	0.9769
123	0.9815	0.9803	0.9807	0.9815	0.9785	0.9805
124	0.9804	0.9776	0.9805	0.9798	0.9774	0.9791
125	0.9783	0.9785	0.9781	0.9784	0.9772	0.9781
126	0.9795	0.9779	0.9789	0.9800	0.9777	0.9788
127	0.9805	0.9803	0.9806	0.9811	0.9789	0.9803
128	0.9827	0.9819	0.9824	0.9822	0.9811	0.9821
129	0.9820	0.9821	0.9819	0.9813	0.9801	0.9815
130	0.9792	0.9810	0.9804	0.9797	0.9779	0.9796
131	0.9778	0.9788	0.9794	0.9787	0.9769	0.9783

Table 5. *Cont.*

Hexagon Size	Test Layer 1	Test Layer 2	Test Layer 3	Test Layer 4	Test Layer 5	Mean
132	***0.9822***	***0.9822***	***0.9843***	***0.9839***	***0.9821***	***0.9829***
133	0.9787	0.9791	0.9795	0.9788	0.9779	0.9788
134	0.9811	0.9819	0.9819	0.9818	0.9808	0.9815
135	0.9829	0.9837	0.9829	0.9825	0.9823	0.9828
136	0.9770	0.9777	0.9776	0.9770	0.9766	0.9772
137	0.9769	0.9769	0.9785	0.9779	0.9767	0.9774
138	0.8902	0.8865	0.8883	0.8855	0.8873	0.8875
139	0.9620	0.9636	0.9612	0.9594	0.9606	0.9614
140	0.9788	0.9803	0.9797	0.9789	0.9772	0.9790
141	0.9754	0.9789	0.9769	0.9756	0.9748	0.9763
142	0.8726	0.8682	0.8738	0.8700	0.8718	0.8713
143	0.8780	0.8749	0.8790	0.8733	0.8760	0.8762
144	0.9730	0.9745	0.9740	0.9737	0.9725	0.9735
145	0.9792	0.9777	0.9788	0.9783	0.9769	0.9782
146	0.9797	0.9795	0.9794	0.9794	0.9772	0.9790
147	0.9774	0.9784	0.9773	0.9777	0.9762	0.9774
148	0.9665	0.9686	0.9665	0.9664	0.9647	0.9665
149	0.9612	0.9619	0.9600	0.9595	0.9586	0.9602
150	0.9756	0.9753	0.9757	0.9767	0.9744	0.9755
151	0.9788	0.9777	0.9784	0.9790	0.9760	0.9780
152	0.9782	0.9781	0.9783	0.9791	0.9759	0.9779
153	0.9775	0.9771	0.9769	0.9778	0.9766	0.9772
154	0.9674	0.9685	0.9659	0.9679	0.9667	0.9673
155	0.9617	0.9628	0.9602	0.9616	0.9604	0.9613
156	0.9747	0.9748	0.9754	0.9744	0.9737	0.9746
157	0.9752	0.9748	0.9753	0.9759	0.9749	0.9752
158	0.9764	0.9752	0.9754	0.9765	0.9752	0.9757
159	0.9776	0.9766	0.9765	0.9773	0.9767	0.9769
160	0.9716	0.9722	0.9712	0.9714	0.9706	0.9714
161	0.9630	0.9641	0.9630	0.9638	0.9619	0.9632
162	0.9575	0.9570	0.9563	0.9569	0.9564	0.9568
163	0.9700	0.9699	0.9715	0.9692	0.9694	0.9700
164	0.9736	0.9726	0.9745	0.9729	0.9723	0.9732
165	0.9713	0.9704	0.9724	0.9723	0.9710	0.9715

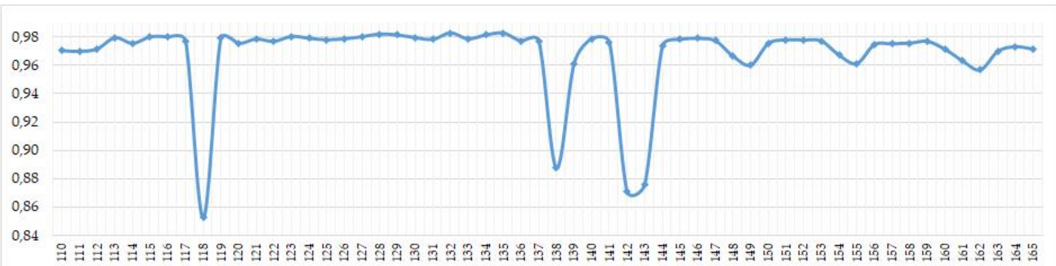

Figure 12. Mean values of Pearson's correlation coefficient, accuracy level 1 km^2. Own elaboration.

By comparing successive values of Pearson's correlation coefficient, one hexagon size was found, for which its value is the highest—132 km^2. The value of the correlation coefficient for the measurement from the third test layer is in this case 0.9843, and the average value for this hexagon size for all five test layers is 0.9829. This is the optimal grid size, to which the data can be generalized without significant decrease in reliability. A hexagon grid with an area of 132 km^2 is shown in the Figure 13, while a map of spatial distribution of non-movable monuments, generalized for this grid is shown in Figure 14.

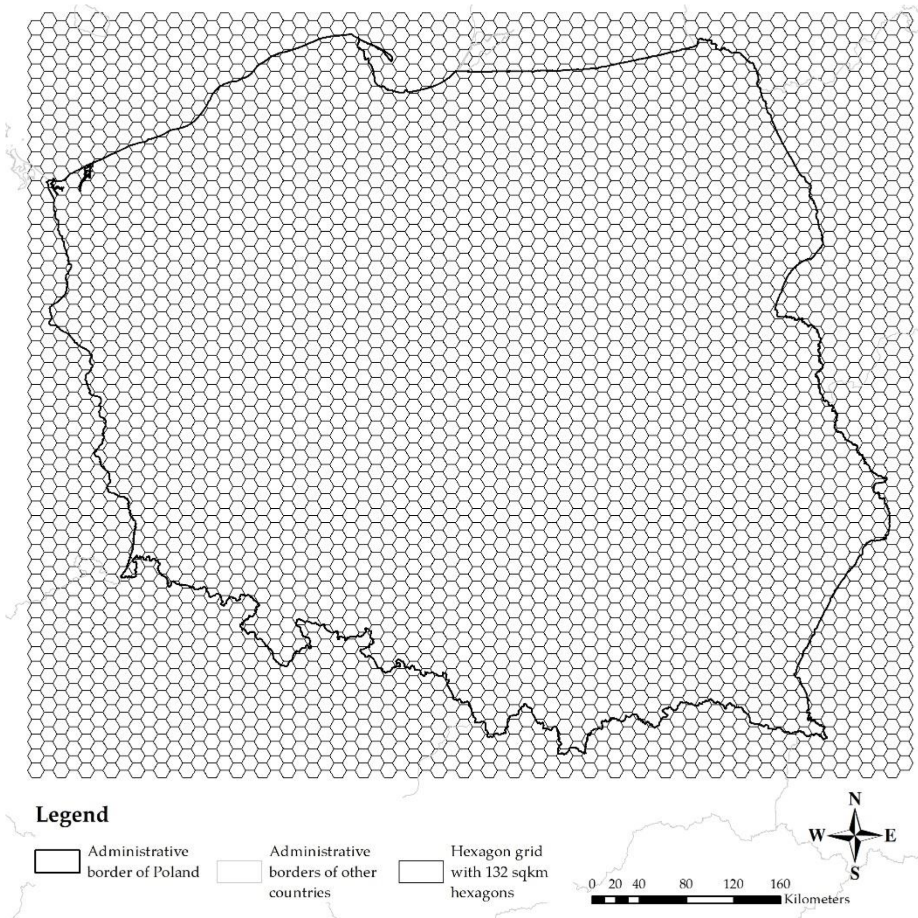

Figure 13. Hexagonal grid with an area of 132 km^2. Own elaboration using ArcMap component of ArcGIS 10.6, on the basis of world data from [27].

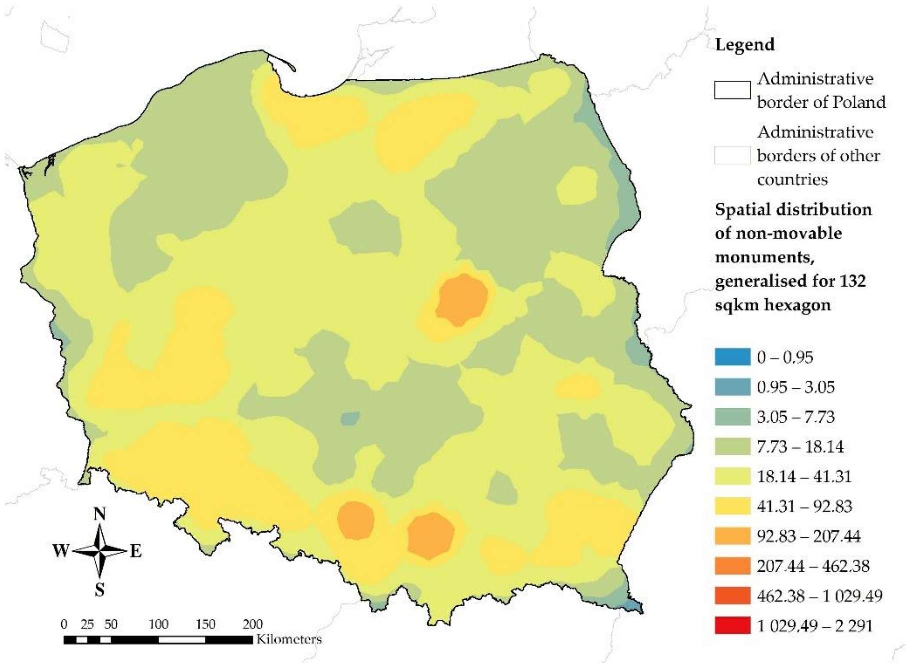

Figure 14. Map of spatial distribution of non-movable monuments, generalized for 132 km^2 hexagon. Own elaboration using ArcMap component of ArcGIS 10.6, on the basis of world data from [27].

4. Discussion

The conducted analyses showed the possibility of using various GIS tools in spatial analysis related to sustainable heritage management. The obtained results allowed us to formulate the following:

1. With the availability of point data containing detailed information about the location of objects, kernel density estimation gives an accurate picture of reality, as shown in the Results section. This is due to the fact that KDE is a non-parametric method, taking into account only the location of objects—not affected by a generalization error.
2. With the availability of point data, which does not contain detailed information about the location of objects, containing only parameters describing it quantitatively, spatial analyses require a different approach. Conducted research has shown that spatial interpolation should be performed; from the methods analyzed in the article, the simple kriging method proved to be optimal. This was confirmed by the smallest RMSE value.
3. In the case of unavailability of point data, the literature analysis showed a solution in the form of data generalization through the use of a hexagonal grid. The research conducted in the article showed that in the range of 110–200 km^2 hexagons, very satisfying results are obtained (Pearson's correlation coefficient assumes values above 0.95). The 132 km^2 hexagon proved to be an optimal one—the Pearson's correlation coefficient after averaging for all five test layers is 0.9829.

5. Conclusions

1. To properly implement sustainable heritage management, thematic maps are required for various related analyses. Development of such maps (as indicated in the article) can be expensive, long, and not always possible to implement based on detailed location data. In the article, using data on non-moveable monuments in Poland, the methodology of creating more generalized maps using less data, is shown. Studies created in Poland (indicated in Conclusions, point 4) often require aggregated maps, without detailed location of the objects. The methodology presented in the article is a response to these needs.
2. The study was based on point data of non-movable monuments in Poland, and the result of the 132 km^2 hexagonal grid is the result only for this specific data. The methodology proposed in the article gives the possibility of universal application. Further research may be based on a comparison of different types of data using the methodology developed in this article. The hexagonal grid gave a specific result, and a comparison of other geometric figures can also become the basis for further studies.
3. The scope of the analysis is also universal. The research in the article was carried out for the area of one country—Poland, including its administrative division units. Similar analyses can be made for any other country with a different administrative division, or even for larger areas (e.g., continents). The scope of the tests may also be limited to a smaller area (e.g., regions).
4. In Poland, some studies on spatial management (part of the sustainable heritage management) directly concern the administrative areas and the analysis closes within its borders. Such documents include: National Spatial Development Concept for the country level; Voivodeship Development Strategy, and Voivodeship Spatial Management Plan for the voivodeship level; and Municipality Development Strategy, Study Of The Conditions And Directions Of The Spatial Management Of Municipality, Local Spatial Management Plans for the municipality level. For such applications, the point level of detail may even be unnecessarily high. Generalization of data may end at the level of a given administrative unit (this is also shown in the article).
5. The research conducted in the article confirmed the wide possibilities of using GIS tools for various purposes, in this particular case concerning cultural heritage, and in particular sustainable heritage management.

Author Contributions: Conceptualization, M.C., K.R., and M.O.; Methodology, M.C., K.R., and M.O.; Formal analysis, M.C., K.R., and M.O.; Writing—original draft preparation, M.C. and K.R.; Writing—review and editing, M.C., K.R., and M.O.; Software, M.C. and M.O.; Visualization, M.C., K.R., and M.O.

Funding: This research received no external funding.

Acknowledgments: Authors would like to thank the National Heritage Board of Poland, for sharing data on non-movable monuments in Poland.

Conflicts of Interest: The authors declare no conflict of interest.

References

1. Alkhalidi, A.; Qoaider, L.; Khashman, A.; Al-Alami, A.R.; Jiryes, S. Energy and Water as Indicators for Sustainable City SiteSelection and Design in Jordan using smart grid. *Sustain. Cities Soc.* **2018**, *37*, 125–132. [CrossRef]
2. Antonopoulos, E. Sustainable Urban Development in Greece Using Integrated Territorial Investments. *Eur. Struct. Investig. Funds J.* **2018**, *6*, 28–34.
3. Bell, S.; Morse, S. *Routledge Handbook of Sustainability Indicators*; Routledge: London, UK, 2018; ISBN 9781138674769.
4. *Act of 27 April 2001 Environmental Protection Law*; Journal of Laws: Warsaw, Poland, 2001; Volume 62.
5. *World Commission on Environment and Development: Our Common Future*; Oxford University Press: Oxford, UK, 1987.
6. Pearce, D.W. Sustainable development and developing country economies. In *Sustainable Environmental Management*; Turner, R.K., Ed.; Bellhaven Press: London, UK, 1993; pp. 70–105.
7. Bogacz-Wojtanowska, E.; Góral, A.; Bugdol, M. The Role of Trust in Sustainable Heritage Management Networks. Case Study of Selected Cultural Routes in Poland. *Sustainability* **2019**, *11*, 2844. [CrossRef]
8. Hawkes, J. *The Fourth Pillar of Sustainability: Culture's Essential Role in Public Planning*; Cultural Development Network: Melbourne, Australia, 2001; ISBN 1 86335 050 0.
9. James, P.; Magee, L.; Scerri, A.; Steger, M. Measuring Community Sustainability: The social Life Questionaire. In *Urban Sustainability in Theory and Practice: Circles of Sustainability*; Routledge: London, UK, 2015; pp. 161–180. ISBN 9781138025721.
10. Soini, K.; Birkeland, I. Exploring the scientific discourse on cultural sustainability. *Geoforum* **2014**, *51*, 213–223. [CrossRef]
11. Janikowski, R. Kultura osią zrównoważonego rozwoju. In *Kultura a Zrównoważony Rozwój*; Janikowski, R., Krzysztofek, K., Eds.; Polski Komitet do spraw UNESCO: Warsaw, Poland, 2009; pp. 17–39. ISBN 9788390293943.
12. Barthel-Boucher, D. Cultural Heritage and the Challenge of Sustainability. *Online J. Public Archaeol.* **2018**, *4*, 163.
13. Hall, S.; Evans, J.; Nixon, S. *Representation. Cultural Representations and Signifying Practices*, 2nd ed.; Sage/Open University: London, UK, 2013; ISBN 9781849205634.
14. Kirshenblatt-Gimblett, B. Intangible heritage as metacultural production. *Mus. Int.* **2014**, *66*, 52–65. [CrossRef]
15. Davies, J.; Whimster, R.; Clayton, L. *Heritage Counts 2009, England*; English Heritage: London, UK, 2009.
16. Boryczka, E.M.; Michalak, J.; Rzeńca, P. Protection of valuable areas of local cultural heritage in sustainable development. Cultural parks in the Lodz region. *Ekon. I Środowisko* **2019**, *1*, 225–240.
17. Pereira Roders, A.; van Oers, R. Editorial: Bridging cultural heritage and sustainable development. *J. Cult. Herit. Manag. Sustain. Dev.* **2011**, *1*, 5–14. [CrossRef]
18. Bonenberg, W. The Role of Cultural Heritage in Sustainable Development. Values and Valuation as Key Factors in Spatial Planning of Rural Areas. In *Advances in Intelligent Systems and Computing Book Series (AISC, Volume 966)*; Springer: Cham, Switzerland, 2019; pp. 124–134.
19. Rzasa, K.; Ogryzek, M.; Kulawiak, M. Cultural Heritage in Spatial Planning. In Proceedings of the 2016 Baltic Geodetic Congress (BGC Geomatics), Gdansk, Poland, 2–4 June 2016; pp. 85–89.
20. Papoulias, E.; Zounis, T.-P. *The Historic and Monumental Enhancement as a Tool for the Sustainable Development of Cultural Assets of Greece*; Springer: Cham, Switzerland, 2019; pp. 271–278.

21. Persson-Fischier, U. Sustainability in conflict: A study of cruise tourism to Gotland. In Proceedings of the MARE People and the Sea X, Amsterdam, The Netherlands, 24–28 June 2019.
22. Ndiaye, M. Barriers to sustainable tourism in Senegal. *Int. J. Innov. Educ. Res.* **2019**, *7*, 258–274. [CrossRef]
23. *Act of 23 July 2003 on the Protection of Monuments and the Guardianship of Monuments*; Journal of Laws: Warsaw, Poland, 2003; Volume 162.
24. *Regulation of the Minister of Culture of 9 February 2004 on the Model of an Information Sign Affixed to Non-Movable Monuments Entered in the Register of Monuments*; Journal of Laws: Warsaw, Poland, 2004; Volume 30.
25. *Final act of the Intergovernmental Conference on the Protection of Cultural Property in the Event of Armed Conflict*; UNESCO: Hague, The Netherlands, 1954; p. 83.
26. Bielak, R.; Głowacka-Smolis, K.; Gustyn, J.; Kozera, A.; Kozłowska, J.; Lipowska, E.; Marikin, M.; Nowak, T.; Pilaszek, K.; Rybak-Nguyen, E.; et al. *Statistical Yearbook of the Republic of Poland 2018*; Statistics Poland: Warsaw, Poland, 2018.
27. Database of Global Administrative Areas, GADM. Available online: https://gadm.org (accessed on 25 July 2019).
28. Head Office of Geodesy and Cartography, Poland. Available online: http://www.gugik.gov.pl/pzgik/dane-bez-oplat/dane-z-panstwowego-rejestru-granic-i-powierzchni-jednostek-podzialow-terytorialnych-kraju-prg (accessed on 25 July 2019).
29. Qi, L.; Huang, J.; Gao, J.; Cui, Z. Modelling the Impacts of Bathymetric Changes on Water Level in China's Largest Freshwater Lake. *Water* **2019**, *11*, 1469. [CrossRef]
30. Yang, B. Developing a Mobile Mapping System for 3D GIS and Smart City Planning. *Sustainability* **2019**, *11*, 3713. [CrossRef]
31. Erdin, C.; Akbaş, H.E. A Comparative Analysis of Fuzzy TOPSIS and Geographic Information Systems (GIS) for the Location Selection of Shopping Malls: A Case Study from Turkey. *Sustainability* **2019**, *11*, 3837. [CrossRef]
32. Layomi Jayasinghe, S.; Kumar, L.; Sandamali, J.; Layomi Jayasinghe, S.; Kumar, L.; Sandamali, J. Assessment of Potential Land Suitability for Tea (*Camellia sinensis* (L.) O. Kuntze) in Sri Lanka Using a GIS-Based Multi-Criteria Approach. *Agriculture* **2019**, *9*, 148. [CrossRef]
33. Xiong, J.; Li, J.; Cheng, W.; Wang, N.; Guo, L.; Xiong, J.; Li, J.; Cheng, W.; Wang, N.; Guo, L. A GIS-Based Support Vector Machine Model for Flash Flood Vulnerability Assessment and Mapping in China. *ISPRS Int. J. Geo-Inf.* **2019**, *8*, 297. [CrossRef]
34. Kartoziia, A. Assessment of the Ice Wedge Polygon Current State by Means of UAV Imagery Analysis (Samoylov Island, the Lena Delta). *Remote Sens.* **2019**, *11*, 1627. [CrossRef]
35. Nohani, E.; Moharrami, M.; Sharafi, S.; Khosravi, K.; Pradhan, B.; Pham, B.T.; Lee, S.; Melesse, A.M. Landslide Susceptibility Mapping Using Different GIS-Based Bivariate Models. *Water* **2019**, *11*, 1402. [CrossRef]
36. Tien Bui, D.; Khosravi, K.; Shahabi, H.; Daggupati, P.; Adamowski, J.F.; Melesse, A.M.; Thai Pham, B.; Pourghasemi, H.R.; Mahmoudi, M.; Bahrami, S.; et al. Flood Spatial Modeling in Northern Iran Using Remote Sensing and GIS: A Comparison between Evidential Belief Functions and Its Ensemble with a Multivariate Logistic Regression Model. *Remote Sens.* **2019**, *11*, 1589. [CrossRef]
37. Kimsey, M.; Page-Dumroese, D.; Coleman, M.; Kimsey, M.; Page-Dumroese, D.; Coleman, M. Assessing Bioenergy Harvest Risks: Geospatially Explicit Tools for Maintaining Soil Productivity in Western US Forests. *Forests* **2011**, *2*, 797–813. [CrossRef]
38. Song, B.; Park, K. Analysis of Spatiotemporal Urban Temperature Characteristics by Urban Spatial Patterns in Changwon City, South Korea. *Sustainability* **2019**, *11*, 3777. [CrossRef]
39. Rząsa, K.; Ogryzek, M.; Ciski, M. Application of GIS technology in the protection of monuments on the example of Historic Monuments. *E3s Web Conf.* **2018**, *63*. [CrossRef]
40. Rząsa, K.; Ciski, M. Archaeological monuments of the Warmian-Masurian voivodeship—Spatial analysis using GIS tools. *E3s Web Conf.* **2018**, *63*. [CrossRef]
41. Rząsa, K.; Ciski, M.; Ogryzek, M. Application of GIS Tools in Spatial Distribution Modeling of Historical Monuments. *Geomat. Environ. Eng.* **2019**, *13*, 61. [CrossRef]
42. Weichselbaum, J.; Papathoma, M. Sharpening census information in GIS to meet real-world conditions—The case for Earth Observation. *Wit Trans. Ecol. Environ.* **2005**, *84*. [CrossRef]
43. Ogryzek, M.; Ciski, M. Cartographic Methods of Presentation the Average Transaction Prices of the Undeveloped Land. *Civ. Environ. Eng. Rep.* **2018**, *28*, 85–100. [CrossRef]

44. Singh, A. Remote sensing and GIS applications for municipal waste management. *J. Environ. Manag.* **2019**, *243*, 22–29. [CrossRef] [PubMed]
45. Peragón, J.M.; Pérez-Latorre, F.J.; Delgado, A.; Tóth, T. Best management irrigation practices assessed by a GIS-based decision tool for reducing salinization risks in olive orchards. *Agric. Water Manag.* **2018**, *202*, 33–41. [CrossRef]
46. Kogure, K.; Takasaki, Y. GIS for empirical research design: An illustration with georeferenced point data. *PLoS ONE* **2019**, *14*, e0212316. [CrossRef] [PubMed]
47. Escobar, F.; Williamson, I. Hierarchical Spatial Reasoning Applied To the Automated Design of Administrative Boundaries Using GIS. In Proceedings of the URISA 2000, Orlando, FL, USA, 19–23 August 2000; pp. 185–200.
48. Estrada-Peña, A.; Venzal, J.M. A GIS framework for the assessment of tick impact on human health in a changing climate. *Geospat. Health* **2007**, *1*, 157–168. [CrossRef]
49. Gullberg, J. *Mathematics: From the Birth of Numbers*; University of Denver: Denver, CO, USA, 1997; ISBN 039304002X.
50. De Sousa, L.; Nery, F.; Sousa, R.; Matos, J. Assessing the accuracy of hexagonal versus square tilled grids in preserving DEM surface flow directions. In Proceedings of the 7th International Symposium on Spatial Accuracy Assessment in Natural Resources and Environmental Sciences, Lisbon, Portugal, 5–7 July 2006; pp. 191–200.
51. Golay, M.J.E. Hexagonal Parallel Pattern Transformations. *IEEE Trans. Comput.* **1969**, *18*, 733–740. [CrossRef]
52. Mersereau, R.M. The processing of hexagonally sampled two-dimensional signals. *Proc. IEEE* **1979**, *67*, 930–949. [CrossRef]
53. He, X.; Shen, G.; Xu, R.; Yang, W.; Zhang, C.; Liu, Z.; Chen, B.; Liu, J.; Song, M. Hexagonal and square patterned silver nanowires/PEDOT:PSS composite grids by screen printing for uniformly transparent heaters. *Polymers* **2019**, *11*, 468. [CrossRef]
54. Uher, V.; Gajdoš, P.; Snášel, V.; Lai, Y.-C.; Radecký, M. Hierarchical Hexagonal Clustering and Indexing. *Symmetry* **2019**, *11*, 731. [CrossRef]
55. Brimkov, V.E.; Barneva, R.P. "Honeycomb" vs Square and Cubic Models. *Electron. Notes Theor. Comput. Sci.* **2001**, *46*, 321–338. [CrossRef]
56. Wen, W.; Khatibi, S. The impact of curviness on four different image sensor forms and structures. *Sensors* **2018**, *18*, 429. [CrossRef] [PubMed]
57. Lee, G.; Chong, N.Y. A geometric approach to deploying robot swarms. *Ann. Math. Artif. Intell.* **2008**, *52*, 257–280. [CrossRef]
58. Snyder, J.P. *Flattening the Earth: Two Thousand Years of Map Projections*; University of Chicago Press: Chicago, IL, USA, 1993; ISBN 9780226767475.
59. Steenmans, C.; Lillethun, A.; Cryan, S.; Bliki, J.; Jessen, T.; Lund, M.; Bredahl, L.; Jeppesen, J. *Guide to Geographical Data and Maps*; European Environmental Agency: Copenhagen, Denmark, 2005.
60. Annoni, A.; Bernard, L.; Lillethun, A.; Ihde, J.; Gallego, J.; Rives, M.; Sommer, E.; Poelman, H.; Condé, S.; Greaves, M.; et al. 1st Workshop on European Reference Grids. In *Proceedings of the 1st European Reference Grid workshop and Proposal for a European Reference Grid Coding System*; Annoni, A., Ed.; JRC-Institute for Environment and Sustainability: Ispra, Italy, 2004.
61. Silverman, B.W. *Density Estimation: For Statistics and Data Analysis*; Routledge: London, UK, 2018; ISBN 9781351456173.
62. Nie, K.; Wang, Z.; Du, Q.; Ren, F.; Tian, Q.; Nie, K.; Wang, Z.; Du, Q.; Ren, F.; Tian, Q. A Network-Constrained Integrated Method for Detecting Spatial Cluster and Risk Location of Traffic Crash: A Case Study from Wuhan, China. *Sustainability* **2015**, *7*, 2662–2677. [CrossRef]
63. Yang, X.; Zhao, Z.; Lu, S. Exploring spatial-temporal patterns of urban human mobility hotspots. *Sustainability* **2016**, *8*, 674. [CrossRef]
64. Qin, Z.; Li, W.; Xiong, X. Estimating wind speed probability distribution using kernel density method. *Electr. Power Syst. Res.* **2011**, *81*, 2139–2146. [CrossRef]
65. Baxter, M.J.; Beardah, C.C.; Wright, R.V.S. Some archaeological applications of kernel density estimates. *J. Archaeol. Sci.* **1997**, *24*, 347–354. [CrossRef]
66. Brigand, R.; Weller, O. Kernel density estimation and transition maps of Moldavian Neolithic and Eneolithic settlement. *Data Brief* **2018**, *17*, 452–458. [CrossRef]

67. Fadda, D.; Slezak, E.; Bijaoui, A. Density estimation with non-parametric methods. *Astron. Astrophys. Suppl. Ser.* **1997**, *127*, 335–352. [CrossRef]
68. Danese, M.; Lazzari, M.; Murgante, B. Kernel Density Estimation Methods for a Geostatistical Approach in Seismic Risk Analysis: The Case Study of Potenza Hilltop Town (Southern Italy). In *Computational Science and Its Applications—ICCSA 2008*; Springer: Berlin/Heidelberg, Germany, 2008; pp. 415–429.
69. Kremer, J.; Gieseke, F.; Steenstrup Pedersen, K.; Igel, C. Nearest neighbor density ratio estimation for large-scale applications in astronomy. *Astron. Comput.* **2015**, *12*, 67–72. [CrossRef]
70. Jang, W.; Hendry, M. Cluster analysis of massive datasets in astronomy. *Stat. Comput.* **2007**, *17*, 253–262. [CrossRef]
71. Vio, R.; Fasano, G.; Lazzarin, M.; Lessi, O. Kernel density estimators applied to gamma ray light curves. *Astron. Astrophys.* **1986**, *289*, 640–648.
72. Worton, B.J. Kernel methods for estimating the utilization distribution in home- range studies. *Ecology* **1989**, *70*, 164–168. [CrossRef]
73. Pittiglio, C.; Skidmorea, A.K.; van Gils, H.A.M.J.; Prins, H.H.T. Identifying transit corridors for elephant using a long time-series. *Int. J. Appl. Earth Obs. Geoinf.* **2012**, *14*, 61–72. [CrossRef]
74. Maxwell, S.M.; Scales, K.L.; Bograd, S.J.; Briscoe, D.K.; Dewar, H.; Hazen, E.L.; Lewison, R.L.; Welch, H.; Crowder, L.B. Seasonal spatial segregation in blue sharks (*Prionace glauca*) by sex and size class in the Northeast Pacific Ocean. *Divers. Distrib.* **2019**. [CrossRef]
75. Niblett, M.; Church, R.; Sweeney, S.; Barber, K.; Niblett, M.R.; Church, R.L.; Sweeney, S.H.; Barber, K.H. Characterizing Habitat Elements and Their Distribution over Several Spatial Scales: The Case of the Fisher. *Forests* **2017**, *8*, 186. [CrossRef]
76. Jeon, J.; Taylor, J.W. Using Conditional Kernel Density Estimation for Wind Power Density Forecasting. *J. Am. Stat. Assoc.* **2012**, *107*, 66–79. [CrossRef]
77. Juban, J.; Fugon, L.; Kariniotakis, G. Probabilistic Short-Term Wind Power Forecasting Based on Kernel Density Estimators. In Proceedings of the European Wind Energy Conference and Exhibition, EWEC 2007, Milan, Italy, 7–10 May 2007.
78. Wang, L.; Chen, Z.; Ma, D.; Zhao, P.; Wang, L.; Chen, Z.; Ma, D.; Zhao, P. Measuring Carbon Emissions Performance in 123 Countries: Application of Minimum Distance to the Strong Efficiency Frontier Analysis. *Sustainability* **2013**, *5*, 5319–5332. [CrossRef]
79. Fan, Z.; Fan, X.; Crosby, M.K.; Moser, W.K.; He, H.; Spetich, M.A.; Shifley, S.R. Spatio-temporal trends of oak decline and mortality under periodic regional drought in the Ozark Highlands of Arkansas and Missouri. *Forests* **2012**, *3*, 614–631. [CrossRef]
80. Stacciarini, J.M.R.; Vacca, R.; Mao, L. Who and where: A socio-spatial integrated approach for community-based health research. *Int. J. Environ. Res. Public Health* **2018**, *15*, 1375. [CrossRef] [PubMed]
81. Wang, J.; Kwan, M.P.; Chai, Y. An innovative context-based crystal-growth activity space method for environmental exposure assessment: A study using GIS and GPS trajectory data collected in Chicago. *Int. J. Environ. Res. Public Health* **2018**, *15*, 703. [CrossRef] [PubMed]
82. Wang, C.-C.; Chang, C.-D.; Jiang, B. Developing a Health Risk Evaluation Method for Triple H. *Int. J. Environ. Res. Public Health* **2019**, *16*, 1168. [CrossRef] [PubMed]
83. Bonato, M.; Parazzini, M.; Chiaramello, E.; Fiocchi, S.; Le Brusquet, L.; Magne, I.; Souques, M.; Röösli, M.; Ravazzani, P.; Bonato, M.; et al. Characterization of Children's Exposure to Extremely Low Frequency Magnetic Fields by Stochastic Modeling. *Int. J. Environ. Res. Public Health* **2018**, *15*, 1963. [CrossRef] [PubMed]
84. Chiu, S.-T. Bandwidth Selection for Kernel Density Estimation. *Ann. Stat.* **1991**, *19*, 1883–1905. [CrossRef]
85. Sheather, S.J.; Jones, M.C. A Reliable Data-Based Bandwidth Selection Method for Kernel Density Estimation. *J. R. Stat. Soc. Ser. B (Methodol.)* **1991**, *53*, 683–690. [CrossRef]
86. Krisp, J.M.; Peters, S.; Murphy, C.E.; Fan, H. Visual Bandwidth Selection for Kernel Density Maps. *Photogramm. Fernerkund. Geoinf.* **2009**, *2009*, 445–454. [CrossRef]
87. Di Piazza, A.; Conti, F.L.; Viola, F.; Eccel, E.; Noto, L.V. Comparative analysis of spatial interpolation methods in the Mediterranean area: Application to temperature in Sicily. *Water* **2015**, *7*, 1866–1888. [CrossRef]
88. Xia, X.; Qi, Q.; Liang, H.; Zhang, A.; Jiang, L.; Ye, Y.; Liu, C.; Huang, Y. Pattern of Spatial Distribution and Temporal Variation of Atmospheric Pollutants during 2013 in Shenzhen, China. *ISPRS Int. J. Geo-Inf.* **2016**, *6*, 2. [CrossRef]

89. Kethireddy, S.R.; Tchounwou, P.B.; Ahmad, H.A.; Yerramilli, A.; Young, J.H. Geospatial interpolation and mapping of tropospheric ozone pollution using geostatistics. *Int. J. Environ. Res. Public Health* **2014**, *11*, 983–1000. [CrossRef]
90. Johnson, B.; Tateishi, R.; Kobayashi, T. Remote sensing of fractional green vegetation cover using spatially-interpolated endmembers. *Remote Sens.* **2012**, *4*, 2619–2634. [CrossRef]
91. Huo, X.-N.; Li, H.; Sun, D.-F.; Zhou, L.-D.; Li, B.-G.; Huo, X.-N.; Li, H.; Sun, D.-F.; Zhou, L.-D.; Li, B.-G. Combining Geostatistics with Moran's I Analysis for Mapping Soil Heavy Metals in Beijing, China. *Int. J. Environ. Res. Public Health* **2012**, *9*, 995–1017. [CrossRef] [PubMed]
92. Chabala, L.M.; Mulolwa, A.; Lungu, O. Application of Ordinary Kriging in Mapping Soil Organic Carbon in Zambia. *Pedosphere* **2017**, *27*, 338–343. [CrossRef]
93. Gharechelou, S.; Tateishi, R.; Sharma, R.; Johnson, B. Soil Moisture Mapping in an Arid Area Using a Land Unit Area (LUA) Sampling Approach and Geostatistical Interpolation Techniques. *ISPRS Int. J. Geo-Inf.* **2016**, *5*, 35. [CrossRef]
94. Jia, Z.; Zhou, S.; Su, Q.; Yi, H.; Wang, J.; Jia, Z.; Zhou, S.; Su, Q.; Yi, H.; Wang, J. Comparison Study on the Estimation of the Spatial Distribution of Regional Soil Metal(loid)s Pollution Based on Kriging Interpolation and BP Neural Network. *Int. J. Environ. Res. Public Health* **2017**, *15*, 34.
95. Zhang, Z.; Sun, Y.; Yu, D.; Mao, P.; Xu, L. Influence of sampling point discretization on the regional variability of soil organic carbon in the Red Soil Region, China. *Sustainability* **2018**, *10*, 3603. [CrossRef]
96. Szcześniak, M.; Piniewski, M. Improvement of Hydrological Simulations by Applying Daily Precipitation Interpolation Schemes in Meso-Scale Catchments. *Water* **2015**, *7*, 747–779. [CrossRef]
97. Curtarelli, M.; Leão, J.; Ogashawara, I.; Lorenzzetti, J.; Stech, J.; Curtarelli, M.; Leão, J.; Ogashawara, I.; Lorenzzetti, J.; Stech, J. Assessment of Spatial Interpolation Methods to Map the Bathymetry of an Amazonian Hydroelectric Reservoir to Aid in Decision Making for Water Management. *ISPRS Int. J. Geo-Inf.* **2015**, *4*, 220–235. [CrossRef]
98. Dysarz, T. Development of RiverBox—An ArcGIS Toolbox for River Bathymetry Reconstruction. *Water* **2018**, *10*, 1266. [CrossRef]
99. Jung, S.-W.; Lee, K.; Cho, Y.-S.; Choi, J.-H.; Yang, W.; Kang, T.-S.; Park, C.; Kim, G.-B.; Yu, S.-D.; Son, B.-S.; et al. Association by Spatial Interpolation between Ozone Levels and Lung Function of Residents at an Industrial Complex in South Korea. *Int. J. Environ. Res. Public Health* **2016**, *13*, 728. [CrossRef]
100. Xi, Y.; Ren, F.; Liang, S.; Zhang, J.; Lin, D.-N.; Xi, Y.; Ren, F.; Liang, S.; Zhang, J.; Lin, D.-N. Spatial Analysis of the Distribution, Risk Factors and Access to Medical Resources of Patients with Hepatitis B in Shenzhen, China. *Int. J. Environ. Res. Public Health* **2014**, *11*, 11505–11527. [CrossRef] [PubMed]
101. Cressie, N. Spatial prediction and ordinary kriging. *Math. Geol.* **1988**, *20*, 405–421. [CrossRef]
102. Li, J.; Heap, A.D. A review of comparative studies of spatial interpolation methods in environmental sciences: Performance and impact factors. *Ecol. Inform.* **2011**, *6*, 228–241. [CrossRef]
103. Hernández-Ceballos, M.Á.; De Felice, L. Air Mass Trajectories to Estimate the "Most Likely" Areas to Be Affected by the Release of Hazardous Materials in the Atmosphere—Feasibility Study. *Atmosphere* **2019**, *10*, 253. [CrossRef]